

Low magnetic field dynamic nuclear polarization using a single-coil two-channel probe

Dinh M. TonThat,^{a)} Matthew P. Augustine,^{b)} Alexander Pines,^{b)} and John Clarke^{a)}
University of California, Berkeley, California 94720 and Materials Sciences Division, Lawrence Berkeley
National Laboratory, Berkeley, California 94720

(Received 15 November 1996; accepted for publication 5 December 1996)

We describe the design and construction of a single-coil, two-channel probe for the detection of low-field magnetic resonance using dynamic nuclear polarization (DNP). The high-frequency channel of the probe, which is used to saturate the electron spins, is tuned to the electron Larmor frequency, 75 MHz at 2.7 mT, and matched to 50 Ω . Low-field, ^1H nuclear magnetic resonance (NMR) is detected through the second, low-frequency channel at frequencies <1 MHz. The performance of the probe was tested by measuring the DNP of protons in a manganese (II) chloride solution at 2.7 mT. At the proton NMR frequency of 120 kHz, the signal amplitude was enhanced over the value without DNP by a factor of about 200. © 1997 American Institute of Physics. [S0034-6748(97)05203-9]

I. INTRODUCTION

Over the past several decades nuclear magnetic resonance (NMR) spectroscopy has been extensively used to study chemical structure and reactivity on the molecular scale.¹ High resolution NMR spectroscopy of liquids and to some extent of solids has evolved into a routine science.² Despite the many technological and experimental advances in this maturing field, however, there has been limited success in the study of nuclei with integer spin and moderately large quadrupole moments, for example,³ ^{14}N , and of polycrystalline and disordered materials with strong dipolar or quadrupolar couplings.^{4,5} In both cases, the spectra tend to be broad and featureless, concealing much of the useful structural information. One option for overcoming this limited resolution is to remove the magnetic field and perform zero-field spectroscopy.⁶ The sharp NMR or nuclear quadrupole resonance (NQR) spectra that result are, unfortunately, obtained with much lower sensitivity. This reduced sensitivity arises in part because the amplitude of the free induction decay (FID) oscillations scales with the magnetization M of the nuclei and hence, as dictated by the Curie susceptibility, as $1/T$; $\omega/2\pi$ is the frequency, and T is the temperature. Furthermore, the voltage induced in the conventional LC resonant circuit by the precessing nuclei is proportional to ωMQ and hence to $\omega^2 Q/T$, where Q is the quality factor.⁷ Thus, over the frequency range of zero-field NMR, 10 Hz–1 MHz, the signal amplitude is typically many orders of magnitude smaller than in conventional NMR at 10 MHz–1 GHz. Some of the loss in signal-to-noise ratio can be recovered by magnetic field cycling techniques^{8–10} or by decreasing the temperature,^{11,12} or by using both.¹³ Another approach to improving the zero-field detection of magnetic resonance has been the application of superconducting quantum interference devices (SQUIDs),¹⁴ which measure the magnetization directly rather than its time derivative. Such techniques can improve the signal-to-noise ratio by many

orders of magnitude under appropriate circumstances. Unfortunately, the investigation of many interesting chemical systems at low field is still out of reach even with SQUID amplifiers, since the spin density can be too low to produce an appreciable magnetization and the relaxation times at 4.2 K can be extremely long. However, in paramagnetic samples^{15–18} one can greatly enhance the signal by using dynamic nuclear polarization (DNP), where the electron-nuclear spin-flip rate dominates the nuclear relaxation.¹

In DNP one typically applies a rotating magnetic field to saturate the electron spins which, in turn, polarize the nuclei by either scalar or dipolar relaxation. In high magnetic fields this enhancement can be as high as 600 for $^1\text{H}-e^-$ systems. DNP is attractive for low-field studies of free-radical systems, since the Zeeman splittings of the electrons are in the radio frequency (rf) region and the nuclear spin transitions are thus at audio frequencies. To carry out low-field DNP, one clearly requires a two-channel probe capable of producing a rotating field to saturate the paramagnetic electrons and an audio frequency field to interrogate the nuclei. Such probes have been used for both continuous wave^{19,20} and pulsed^{21,22} DNP. These designs usually involve crossed-coil geometries to minimize the effect of the applied rf fields on the low-frequency detection electronics. A drawback to this approach, however, is that the Helmholtz coils typically used are inefficient compared with solenoids of comparable volume. With a pulsed technique one is not forced into a crossed coil arrangement because the electron saturation and FID detection can occur at two different times, as in a gated nuclear Overhauser experiment.²³ In this article we describe the design and performance of a two-channel probe involving a single coil, an actively switched duplexer, and a spectrometer suitable for pulsed DNP at low fields. The chief advantage of the single solenoid design, compared with crossed Helmholtz coils, is that more of the applied rf power is delivered to the sample. By leaving the coil untuned we can study a wide range of nuclear resonance frequencies. Although these experiments were performed at room temperature, the ultimate goal of this work is to incorporate this

^{a)}Department of Physics.

^{b)}Department of Chemistry.

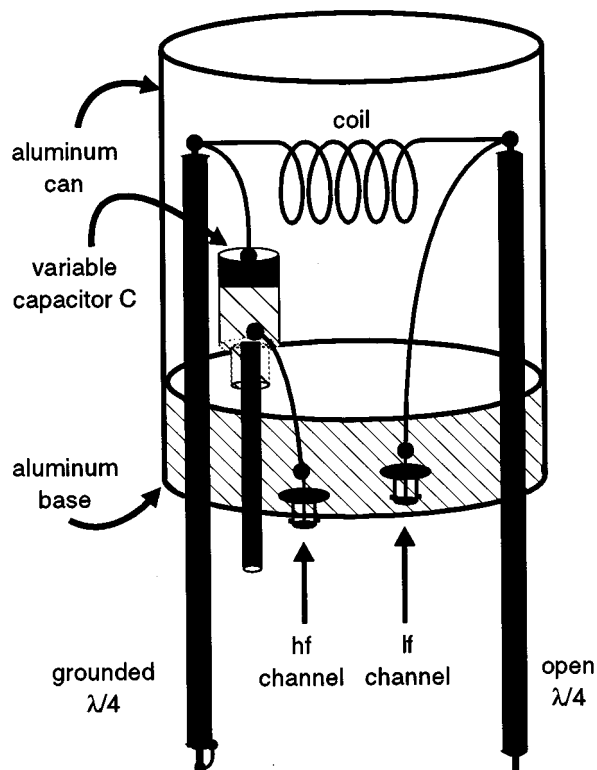


FIG. 1. Configuration of the two-channel probe showing positions of the various components.

design into our pulsed SQUID spectrometer operating at 4.2 K.²⁴

II. EXPERIMENTAL CONFIGURATION

A. Probe

The probe head shown in Fig. 1 is based largely on an earlier double resonance design.²⁵ The circuit consists of an eight-turn solenoid, 22 mm long and 14 mm in diameter, in series with a Polyflon variable capacitor (5–25 pF) for matching, and two quarter-wavelength ($\lambda/4$) coaxial cables. The coil is wound from enameled copper wire (1.27 mm diameter) and has an inductance of 0.69 μH and a volume of about $3.4 \times 10^3 \text{ mm}^3$. The two $\lambda/4$ lines consist of 50 Ω semi-rigid coaxial cable with an outer diameter of 6 mm. The whole assembly is attached to a 25 mm thick, 72-mm-diam aluminum base and enclosed in a cylindrical aluminum can (Fig. 1). This geometry allows us to perform diagnostic tests in our Oxford Instruments 7.04 T superconducting solenoid magnet, which has an 89 mm room temperature bore. We adjusted the number of turns on the coil so that it was self-resonant at 75 MHz, the electron Larmor frequency at a magnetic field of 2.7 mT. We set the series capacitor C to match the circuit to 50 Ω at 75 MHz, and adjusted the length of the coaxial lines to be $\lambda/4$ at that frequency. The open line at the high frequency (hf) provides a path to ground for the coil while at the low frequency (lf) it has no effect since its impedance is high. The closed line behaves in the opposite way. Its impedance at hf is large, and has a negligible effect on the tuned circuit, while at lower frequencies (<1 MHz)

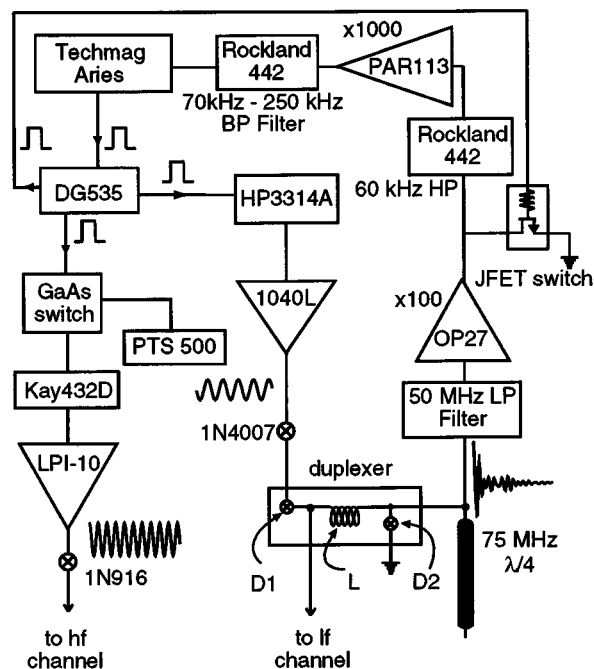


FIG. 2. Configuration of the spectrometer.

the shorted cable grounds the coil. The fact that the lf channel is not a tuned and matched circuit, at first glance, may appear to be a poor choice since a tuned circuit would enhance the voltage by a factor Q . However, as we see in the next section, the corresponding loss in signal is more than compensated by the increased lf bandwidth and the fact that the inductively dominated circuit can easily be coupled to an actively switched duplexer.

B. Spectrometer and duplexer

A block diagram of our spectrometer and duplexer is shown in Fig. 2. The pulse gating and data digitization are accomplished by a Techmag Aries pulse programmer. The timing within a given pulse sequence is determined by a Stanford Research Systems DG 535 pulse generator. The logic output of this unit controls both the hf and lf channels, and a JFET switch. hf pulses at about 75 MHz are produced by switching the output of a PTS-500 oscillator with a GaAs-based rf switch (~ 9 ns ON/OFF). After passing through a Kay 432D variable attenuator, the pulses are amplified by an ENI LPI-10 amplifier to power levels up to 1.5 kW (into 50 Ω). The noise of the amplifier in the absence of pulses is minimized by connecting the output to the hf probe channel via a set of series crossed diodes (1N916) (Fig. 2). The high power (~ 500 W, 50 Ω) lf pulses are produced by amplifying the output of an HP 3314A frequency synthesizer with an ENI 1040L amplifier. A set of series crossed diodes (1N4007) between the amplifier and the probe minimizes amplifier noise during data acquisition.

The action of the spectrometer is as follows. During the hf pulse, the two $\lambda/4$ lines (Fig. 1) ensure that little energy is coupled into the lf channel; any such leakage is attenuated by a third, open $\lambda/4$ line and a passive, 50 MHz low pass filter, with a 35 dB attenuation at 75 MHz, that follow the du-

plexer. After the hf pulse is turned off, the lf pulse is turned on and is isolated from the detection circuit in the following way. During the pulse, diode D1 turns on, providing a low-impedance path (about 0.3Ω) to the probe channel. The diode D2 also turns on and, together with the inductance L of the duplexer ($1.3 \mu\text{H}$) limits the output of the duplexer to about 0.7 V rms . Further attenuation of the lf pulse is provided by the MTO55EL JFET in Fig. 2, which is switched to ground during the lf pulse. After the lf pulse is removed, diodes D1 and D2 turn off, and the FID signal is coupled via the inductor L and low pass filter to the OP27 amplifier. The signal is high pass filtered at 60 kHz by a Rockland 442 filter, amplified by a PAR 113 amplifier and passed through a ($70\text{--}250 \text{ kHz}$) bandpass filter before being digitized by the Techmag.

A static magnetic field up to 20 mT could be applied by means of a solenoid 0.3 m in diameter and 0.6 m long, driven by an HP 6253 A power supply. The field at the center of this magnet was calibrated using electron paramagnetic resonance in a single crystal of the radical cation salt fluoranthene antimony hexafluoride.²⁶

III. RESULTS AND DISCUSSION

A. Performance

Two important criteria for the probe are the isolation of the two channels from each other and the amplitude B_1 of the rf magnetic field for a given input rf power. We determined the channel isolation by connecting each input of the probe in turn to a source at the appropriate frequency and measuring the signal leakage at the other input. The hf isolation, 51 dB , is determined largely by the accuracy ($\sim 1\%$) with which we can adjust the length of the two coaxial lines. The lf isolation (80 dB) is determined by the high impedance of the matching capacitor and the low impedance of the grounded $\lambda/4$ line. Although the length of this line is not important for the lf isolation, significant departures of its length from $\lambda/4$ at the high frequency can result in substantial heating since the hf is not totally reflected. Thus, it is highly advantageous to adjust the length of the line as accurately as possible to $\lambda/4$ since the rf energy is then converted entirely into magnetic field rather than heat.

We determined the amplitude B_1 of the 75 MHz field using the ^{79}Br line in powdered potassium bromide at 7.04 T . At an rf power setting that delivered 1.1 kW into a 50Ω load, the 90° pulse length t_{90} was $5 \mu\text{s}$, yielding $B_1 = 1/4 \gamma_{\text{Br}} t_{90} = 0.65 \text{ mT}$; γ_{Br} is the gyromagnetic ratio for ^{79}Br . We obtained a rough estimate of B_1 in the lf channel by measuring the voltage V_0 from a solenoid with $n=6$ turns and a diameter $d=5 \text{ mm}$ placed inside the coil in Fig. 1. At low frequencies, we estimate B_1 as $4V_0/n\pi d^2\omega$, where ω is the angular frequency. For example, for $V_0=20 \text{ mV}$ and $\omega/2\pi=120 \text{ kHz}$, we find $B_1 \approx 0.2 \text{ mT}$. Subsequently, we refined this value by measuring the 90° pulse length of protons following a gated DNP experiment on the manganese (II) chloride and water solution ($\text{MnCl}_2/\text{H}_2\text{O}$) discussed below. This measurement yielded $t_{90}=50 \mu\text{s}$ and hence $B=0.12 \text{ mT}$.

It is worth pointing out that in principle one could in-

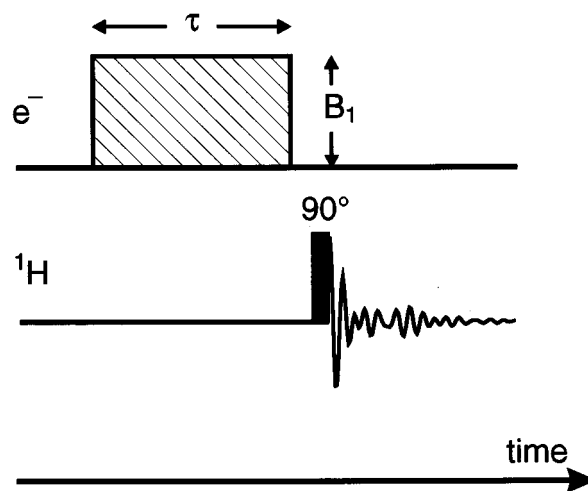


FIG. 3. Pulse sequence: The shaded area is 75 MHz pulse to saturate the electrons, and the 90° pulse is at 120 kHz to excite the protons.

crease the low-frequency value of B_1 by tuning the lf probe channel and matching it to 50Ω . Unfortunately, the large tuning capacitor that would be required to give a reasonably wide tuning range makes this approach somewhat impractical. A further drawback to tuning the lf circuit is that the duplexing strategy adopted here would no longer function, and a more elaborate detection method would have to be used. For these reasons and because lf power is not at a premium in these experiments, we did not attempt to tune the lf channel.

B. Pulsed DNP

We chose to study DNP in a $5 \text{ mM MnCl}_2/\text{H}_2\text{O}$ solution primarily because the $\Delta F=0$, $\Delta m_F = \pm 1$ hyperfine transition energies in $[\text{Mn}(\text{H}_2\text{O})_6]^{2+}$ at $B_0=2.7 \text{ mT}$ are nearly that of the free electron Larmor frequency.²⁷ Furthermore, the dynamics of this system have been well documented.²⁸ The pulse sequence (Fig. 3) consists of an hf pulse of variable magnetic field amplitude B_1 and length τ to saturate the electron spins followed by a 90° lf pulse to interrogate the protons.

The ^1H spectra obtained at constant $B_1=0.65 \text{ mT}$ and for variable τ are shown in Fig. 4; each spectrum is averaged over 400 pulses. The frequency of the electron resonance, 75 MHz , the amplitude and length of the 90° pulse and the frequency of the ^1H NMR line, 120 kHz , are all consistent with one's expectations for a magnetic field of 2.7 mT . The characteristic rise time of the ^1H signal ($T_1=7.3 \text{ ms}$) is also consistent with the T_1 values (10 ms) obtained from the literature.²⁸

The spectra obtained for $\tau=20 \text{ ms}$ and for variable B_1 are shown in Fig. 5, where each spectrum is again the result of 400 acquisitions. The increase of the ^1H amplitude with hf magnetic field from 0.12 to 0.89 mT is consistent with previous continuous wave experiments.²⁹

We note that the data shown in Figs. 4 and 5 do not represent the ultimate enhancement that one could expect from $e^- - ^1\text{H}$ DNP. The amplitude of the ^1H spectra did not saturate with respect to time (Fig. 4) or hf power (Fig. 5).

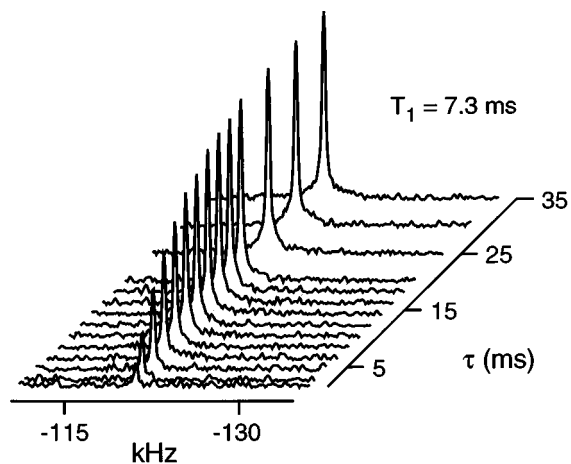


FIG. 4. ^1H spectra observed at $B_0=2.7$ mT vs τ . Each spectrum was averaged over 400 pulses. The inferred T_1 is 7.3 ms.

Unfortunately, the ranges of hf pulse time and amplitude we could explore were at the upper limit of the capability of the ENI LPI-10 pulse amplifier: both longer times and higher powers caused the amplifier to shut down. Clearly, an amplifier capable of delivering more rf energy would yield larger signals. Nevertheless, even with the limited power available, we obtained substantial DNP enhancements. Figure 6(a) shows the ^1H spectrum for 250 000 acquisitions without electron saturation at $B_0=2.7$ mT, while Fig. 6(b) shows the spectrum obtained after 400 acquisitions with an hf pulse of 20 ms at $B_1=0.65$ mT. The signal-to-noise (S/N) ratio was improved from 7.4 to 54.1, while the number of pulses in the average was reduced by a factor of 625. Taking into account the number of scans, we see that the amplitude enhancement due to DNP was 183. By comparison, using a two-coil continuous wave technique, Codrington and Bloembergen²⁸ achieved an enhancement of about 60 for the same value of B_1 .

The large bandwidth of the lf channel allowed us to examine the effect of the static magnetic field on the DNP. In this experiment we adjusted B_0 and the frequency of the 90°

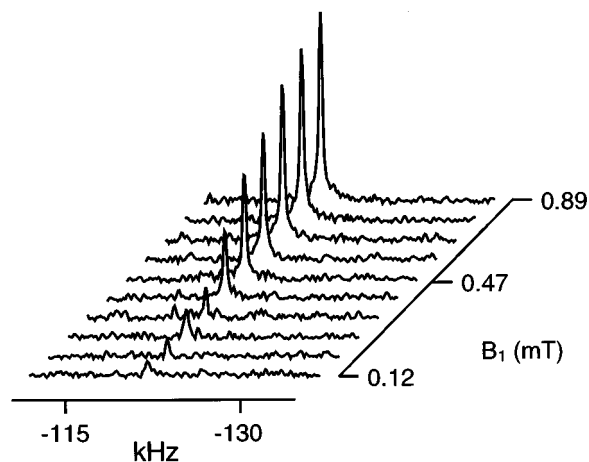


FIG. 5. ^1H spectra observed at $B_0=2.7$ mT vs magnetic field amplitude B_1 of rf pulse. Each spectrum was averaged over 400 pulses. Note B_1 scale is logarithmic.

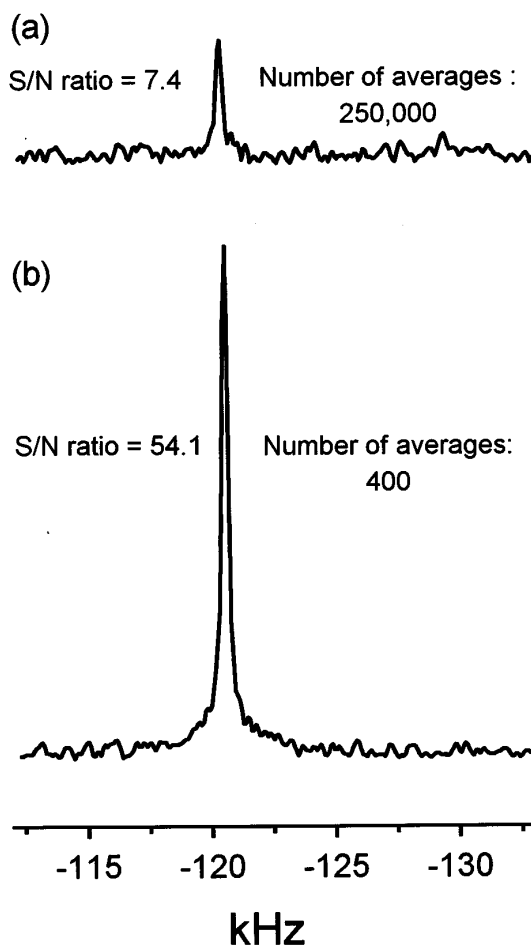


FIG. 6. Comparison of the ^1H spectra at $B_0=2.7$ mT (a) without and (b) with DNP. The enhancement due to DNP is 183.

pulse so that the protons remained on resonance, and left the hf fixed at 75 MHz. The field dependence of the DNP measured in this way was unexpectedly broad. For example, substantially enhanced proton polarization persisted for proton Larmor frequencies of at least 250 kHz, implying that the electron full width bandwidth is at least 150 MHz.

We are currently using this design in a probe for pulsed NMR and NQR using a SQUID amplifier at 4.2 K, where we hope that DNP will both reduce the relaxation time and enhance the signal amplitude of quadrupolar nuclei.

ACKNOWLEDGMENTS

We thank C. S. Yannoni for providing the single-crystal FARC sample for field calibration and Gerard Chingas for many helpful discussions. MPA thanks the National Science Foundation for a postdoctoral fellowship, No. CHE-9504655. This work was supported by the Director, Office of Energy Research, Office of Basic Energy Sciences, Materials Sciences Division of the U.S. Department of Energy under Contract No. DE-AC03-76SF00098.

- ¹A. Abragam, *Principles of Nuclear Magnetism* (Oxford Science, New York, 1989).
- ²R. R. Ernst, *Principles of Nuclear Magnetic Resonance in One and Two Dimensions* (Oxford Science, New York, 1992).
- ³M. Witanowski, L. Stefaniaky, and G. A. Webb, in *Annual Reports on NMR Spectroscopy*, edited by G. A. Webb (Academic, New York, 1993), p. 1.
- ⁴A. M. Portis, *Phys. Rev.* **91**, 1971 (1953).
- ⁵M. M. Maricq and J. S. Waugh, *J. Chem. Phys.* **70**, 3300 (1979).
- ⁶D. P. Weitekamp, A. Bielecki, D. Zax, K. Zilm, and A. Pines, *Phys. Rev. Lett.* **50**, 1807 (1983).
- ⁷E. Fukushima and S. Roeder, *Experimental Pulse NMR a Nuts and Bolts Approach* (Addison-Wesley, Reading, MA, 1981).
- ⁸N. F. Ramsey and R. V. Pound, *Phys. Rev.* **81**, 278 (1951).
- ⁹R. Blinc, *Adv. Nucl. Quad. Reson.* **2**, 71 (1975).
- ¹⁰D. T. Edmonds, *Phys. Rep.* **29**, 233 (1977).
- ¹¹M. S. Conradi, *Concepts Magn. Reson.* **5**, 243 (1993).
- ¹²Y. W. Kim, W. L. Earl, and R. E. Norberg, *J. Magn. Reson.* **116**, 139 (1995).
- ¹³E. R. Slusher and E. L. Hahn, *Phys. Rev.* **166**, 332 (1968).
- ¹⁴J. Clarke, in *The Superconducting Electronics*, edited by H. Weinstock and R. W. Ralston (Kluwer Academic, The Netherlands, 1993), p. 123.
- ¹⁵R. Bates, *Magn. Reson. Rev.* **16**, 237 (1993).
- ¹⁶A. Overhauser, *Phys. Rev.* **89**, 689 (1953).
- ¹⁷A. Abragam, J. Combrisson, and I. Solomon, *Compt. Rend.* **245**, 157 (1957).
- ¹⁸A. Landesman, *Compt. Rend.* **246**, 1538 (1958).
- ¹⁹J. Potenza, *Adv. Mol. Relaxation Processes* **4**, 229 (1972).
- ²⁰N. Chandrakumar and P. T. Narashimhan, *Rev. Sci. Instrum.* **52**, 533 (1981).
- ²¹T. Guiberteau and D. Grucker, *J. Magn. Reson. Ser. A* **105**, 98 (1993).
- ²²D. Grucker, T. Guiberteau, B. Eclancher, J. Chambron, R. Chiarelli, A. Rassat, G. Subra, and B. Gallez, *J. Magn. Reson. B* **106**, 101 (1995).
- ²³A. Derome, *Modern NMR Techniques for Chemistry Research* (Pergamon, New York, 1993).
- ²⁴D. M. TonThat and J. Clarke, *Rev. Sci. Instrum.* (in press).
- ²⁵V. Cross, R. Hester, and J. Waugh, *Rev. Sci. Instrum.* **47**, 1486 (1976).
- ²⁶E. Dormann, G. Sachs, W. Stocklein, B. Bail, and M. Schworer, *Appl. Phys. A* **30**, 227 (1983).
- ²⁷M. Tinkham, R. Weinstein, and A. F. Kip, *Phys. Rev.* **84**, 848 (1951).
- ²⁸R. S. Codrington and N. Bloembergen, *J. Chem. Phys.* **29**, 600 (1958).
- ²⁹A. Overhauser, *Phys. Rev.* **92**, 411 (1953).